Effect of Confinement on Polymer Segmental Motion and Ion Mobility in PEO/Layered Silicate Nanocomposites

M. M. Elmahdy,[†,‡] K. Chrissopoulou,[§] A. Afratis,[§] G. Floudas,*[,†,‡] and S. H. Anastasiadis*[,§,||,⊥]

Department of Physics, University of Ioannina, 451 10 Ioannina, Greece; Biomedical Research Institute, Foundation for Research and Technology-Hellas, P.O. Box 1186, 451 10 Ioannina, Greece; Institute of Electronic Structure and Laser, Foundation for Research and Technology-Hellas, P.O. Box 1527, 711 10 Heraklion Crete, Greece; Department of Physics, University of Crete, 710 03 Heraklion Crete, Greece; and Department of Chemical Engineering, Aristotle University of Thessaloniki, 541 24 Thessaloniki, Greece

Received April 13, 2006

Revised Manuscript Received June 21, 2006

The behavior of polymer fluids in restricted space can be very different from that in the bulk, especially when the molecules are confined to dimensions comparable to their sizes. The dynamics of macromolecules in thin films or in porous media has attracted the scientific interest for more than a decade with the general trends in the data and the outstanding issues highlighted in a number of reviews.[1−5] There has been considerable experimental evidence for significant reductions in the glass transition temperature, T_g, of thin polymer films with decreasing film thickness, indicative of enhanced segmental motion. It is recognized that a free surface and/or a nonwetting hard interface play the key role in these effects,[6,7] whereas a strongly attractive surface may alter the behavior. The effects of confinement on the motion of entire macromolecules are less clear[2,5] and are not further discussed herein.

Besides planar polymer films, other experimental geometries have been utilized to study the effect of confinement on the segmental motion. Dispersion of polymer nanospheres in a medium[8] or of nanoparticles in polymer matrices[9] have been used likewise. The equivalence in the behavior between polymer nanocomposites and thin polymer films has recently been quantitatively verified for silica/polystyrene nanocomposites.[10] Utilizing polymer/layered silicate nanocomposites has been proven particularly advantageous in this respect. Mixing polymers with layered silicates leads to the formation of organic/inorganic hybrids with enhanced properties.[11] Three different types of structures can be identified in these systems: the phase-separated microcomposites, where polymer and silicate are immiscible, the intercalated nanocomposites, where the polymer chains reside between the layers of the inorganic material forming 0.8−2.5 nm thin films, and the exfoliated ones, where the silicate layers are dispersed in the polymer matrix.[12] The intercalated nanohybrids are especially interesting since they offer the opportunity to investigate the static and dynamic properties of macromolecules in nanoconfinement utilizing, however, macroscopic samples and conventional analytical techniques.[13−17]

The segmental motion of poly(methylphenylsiloxane), PMPS, in intercalated nanocomposites, with PMPS confined within the 1.5−2.0 nm spacing between organically modified silicates, was studied by dielectric spectroscopy.[15] Very fast dynamics was observed in confinement with a very weak, yet non-Arrhenius, temperature dependence that extends well below the bulk polymer T_g. At the same time, quasi-elastic neutron scattering showed a significant acceleration of the effective mean-square displacement in confinement[17] near the bulk PMPS T_g. Quadrupole spin-echo ^{2}H NMR on polystyrene/organosilicate hybrids showed a wide distribution of relaxation times whereas Si−H cross-polarization NMR attributed the fast relaxations to segments located near the middle of the 2 nm layer.[16]

Hydrophilic polymers, like poly(ethylene oxide), PEO, can intercalate within hydrophilic silicates such as sodium or lithium montmorillonite, Na^+MMT or Li^+MMT. These materials, in which a polymer electrolyte/cation system is confined between inorganic layers, exhibit interesting electromechanical responses, rendering them potential candidates for applications as electrolytes in solid-state batteries.[18] Investigation of PEO intercalated within Li^+MMT by solid-state ^{2}H NMR[13] and thermally stimulated depolarization current[14] revealed rich dynamics over a broad temperature range with fast relaxing segments existing even at such low temperatures where the bulk PEO shows a completely solidlike response. Moreover, an increase of ionic conductance at room temperature was observed in PEO/Li^+-MMT[18,19] when compared to more conventional PEO/Li^+BF_4 systems.

In this paper, a dielectric spectroscopy investigation is presented, aiming to probe the role of nanoconfinement on both the polymer and the cation dynamics utilizing intercalated polymer/layered silicate nanocomposites with ∼1 nm PEO films residing within the galleries of hydrophilic Na^+MMT. Confinement results in a speed-up of the PEO segmental relaxation dynamics, which display an Arrhenius temperature dependence and persist for temperatures much lower than the bulk T_g. Moreover, the ionic mobility is found to be enhanced in the nanocomposites.

PEO/Na^+MMT nanocomposites were synthesized by direct melt mixing of PEO homopolymer (M_w = 100 000, T_g = −67 °C and T_m = 65 °C, Aldrich) with Na^+MMT (Southern Clay) in compositions that covered the range from pure polymer to pure clay. The presence of hydrated Na^+ makes the galleries hydrophilic so that polar polymers can mix without the need of modification of the silicate hosts. The two components were mixed in the appropriate amounts, grinded in a mortar to get a fine powder, annealed in a vacuum oven at 100 °C for 2 days, grinded again, and pressed in a form of a pellet. The structure of the hybrids was investigated by X-ray diffraction (RINT-2000 Rigaku diffractometer; 12 kW rotating anode generator, Cu Kα radiation, λ = 1.54 Å), polarizing optical microscopy (POM), and differential scanning calorimetry (DSC). Figure 1 shows the X-ray diffraction patterns for the pure components and the nanohybrids. The pure Na^+MMT shows a main (001) diffraction peak at $2\theta = 8.8°$, which corresponds to an interlayer spacing of 1.0 nm. As the PEO concentration increases, the Na^+-MMT diffraction peak disappears and two other peaks emerge at 6.8° and 4.8° that correspond to interlayer distances of 1.30

[†] University of Ioannina.
[‡] Biomedical Research Institute, Foundation for Research and Technology-Hellas.
[§] Institute of Electronic Structure and Laser, Foundation for Research and Technology-Hellas.
[||] University of Crete.
[⊥] Aristotle University of Thessaloniki.
* Corresponding authors. E-mail: spiros@iesl.forth.gr; gfloudas@cc.uoi.gr.

10.1021/ma0608368 CCC: $33.50
Published on Web 07/06/2006

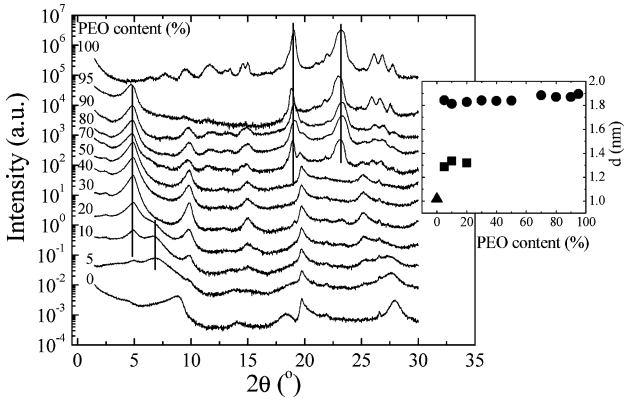

Figure 1. Wide-angle X-ray diffraction patterns for the PEO/Na^+MMT nanocomposites as a function of PEO content (weight percent). The lines indicate the interlayer distances of galleries composed of single and double layers of PEO (at low angles) and the characteristic peaks of monoclinic PEO. The inset shows the interlayer distance, d_{001}, of Na^+MMT (▲) and nanocomposites with single (■) and double (●) layers of PEO.

and 1.85 nm and whose relative intensities depend on the PEO content. At concentrations up to 20 wt %, the PEO chains within the galleries form either a single- or a double-layer structure of disordered liquidlike chains, in accordance with simulation results.[19] Further increase of the PEO concentration reveals only double layers of intercalated PEO chains. Moreover, for PEO content below 70 wt % no peaks are observed that can be assigned to the crystalline structure of PEO. Indeed, DSC and POM measurements on these hybrids reveal that the PEO chains remain amorphous, in agreement with the XRD data. It is only for PEO concentrations higher than 70 wt % that two peaks at 18.9° and 23.2° emerge, which agree with the diffraction peaks of bulk PEO due to its monoclinic crystal structure (with a unit cell parameter of 1.93 nm along the helix axis). This indicates crystallization of the excess polymer outside the completely full galleries.

Dielectric spectroscopy (DS) was used to investigate the collective dynamics of PEO in the frequency range $10^{-2}-10^6$ Hz (Novocontrol BDS with a Solatron-Schlumberger frequency response analyzer FRA 1260). The measured complex dielectric permittivity, $\epsilon^*(\omega) = \epsilon'(\omega) - i\epsilon''(\omega)$, is given by the one-sided Fourier transform of the time derivative of the dipole−dipole correlation function $C(t)$; for nonzero dipole moment perpendicular to the chain contour, $C(t)$ probes local motions. The sample was residing between two gold-plated stainless steel electrodes (diameter 20 mm) in a cryostat. The $\epsilon^*(\omega)$ data were analyzed with the empirical Havriliak−Negami (HN) function $\epsilon^*(\omega) = \epsilon_\infty + \Delta\epsilon/[1 + (i\omega\tau_{HN})^\alpha]^\gamma$, where τ_{HN} is the characteristic relaxation time, $\Delta\epsilon = \epsilon'_0 - \epsilon'_\infty$ is the relaxation strength of the process, and α, γ ($0 < \alpha, \alpha\gamma \leq 1$) describe the symmetric and asymmetric broadening of the distribution of relaxation times. An additional ionic conductivity contribution at low frequencies and high temperatures is accounted for by an ω^{-1} dependence. Alternatively, the electric modulus, M^*, representation of the dielectric data was used, where $M^*(\omega) = 1/\epsilon^*(\omega)$; this allows extracting the ionic mobility in addition to the polymer mobility. Herein we have employed analysis in both representations, but the reported relaxation times are from the M^* representation.[20] Note that in the analysis of both ϵ^* and M^* the fitting procedure involved fitting the β-relaxation at low temperatures to a single Havriliak−Negami process and extracting the shape and dielectric strength parameters. At higher temperatures, both the α'- and α-processes (see below) were fitted using fixed shape parameter γ ($\gamma = 1$) for both processes together with the shape parameters for the β-process obtained at low temperatures.

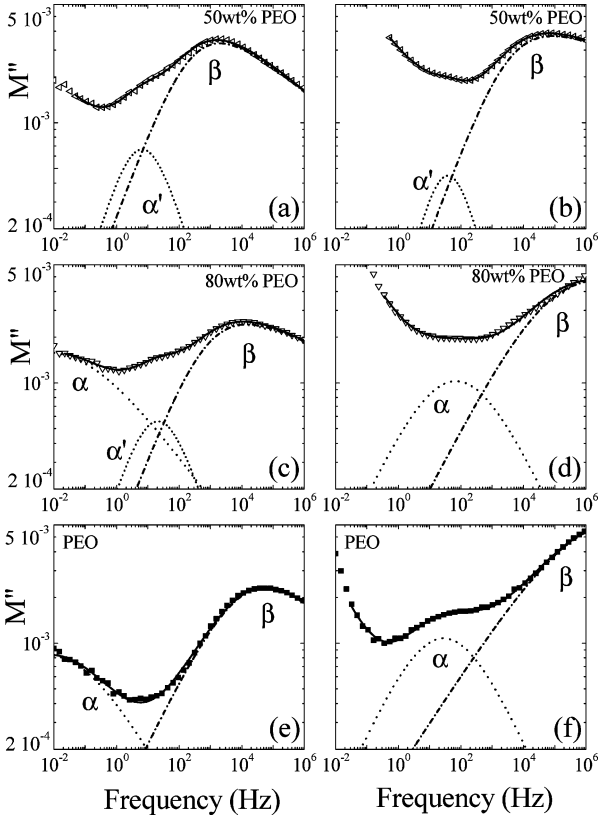

Figure 2. Imaginary part of the electric modulus for the PEO/Na^+-MMT composites with PEO weight content of 50% at $T = 183$ K (a; upper left) and $T = 223$ K (b; upper right), 80% at $T = 193$ K (c; middle left) and $T = 235$ K (d; middle right), and for pure PEO at $T = 193$ K (e; lower left) and $T = 233$ K (f; lower right). The processes needed for the deconvolution of the spectra are shown with dash−dotted (β), dashed (α'), and dotted (α) lines, whereas the solid lines are the summations of the processes (together with the conductivity at high temperatures, which is not shown).

Figure 2 shows representative plots of the imaginary part of the electric modulus, $M''(\omega)$, as a function of frequency for pure PEO and two different PEO/MMT nanohybrids at a pair of temperatures. At these temperatures, a local β-process and a segmental α-process are evident in the spectrum of bulk PEO (Figure 2e,f). A process appears, however, in the nanocomposites at intermediate frequencies (Figure 2a−c), which is termed α'; this process is present in all composite spectra (together with the β-process) whereas the α-process is observed only in the polymer-rich composites, i.e., in nanohybrids with both intercalated and in-excess PEO chains outside the galleries (e.g., for the 80 wt % hybrid in Figure 2c,d). The various processes are illustrated in Figure 2 together with the complete fit to the $M''(\omega)$ data.

The most probable relaxation times of the PEO/Na^+MMT hybrids with 50, 70, and 80 wt % PEO are shown in Figure 3 as exemplary cases of the rich nanocomposite dynamics. The solid line corresponds to the α-process and the dashed one to the β-process of pure PEO. The relaxation times of the α-process for bulk PEO conform to the Vogel−Fulcher−Tammann (VFT) equation $\tau = \tau_0 \exp[B/(T - T_0)]$, with $\tau_0 = 1.0 \times 10^{-11}$ s the high-temperature intercept, $B = 2700 \pm 300$ K the activation parameter, and $T_0 = 112 \pm 10$ K the "ideal" glass transition temperature. The relaxation times for the β-process of the pure PEO follow an Arrhenius dependence $\tau = \tau_0 \exp[E/RT]$ with a single activation energy $E = 35 \pm 0.5$ kJ/mol and a $\tau_0 = 6 \times$

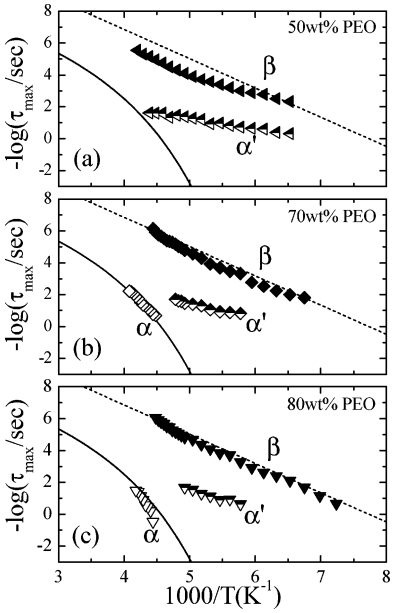

Figure 3. Arrhenius relaxation map for the PEO/Na^+MMT nanocomposites with 50 wt % (a), 70 wt % (b), and 80 wt % (c) PEO. The β-process (filled symbols), the α'-process (half-filled symbols), and the α-process (open symbols) in the composites are shown together with the α-process (solid line) and β-process (dashed line) for bulk PEO. The error bars are comparable to the size of the symbols.

10^{-15} s characteristic of a local process (R is the gas constant). For the 50 wt % hybrid as well as for all hybrids with lower PEO content, the usual PEO α-process is not observed at all. The PEO segments are all confined within the galleries and relax with the faster α'-process, which exhibits an Arrhenius temperature dependence with a single activation energy. The fast local β-process is observed with a rate comparable to that of bulk PEO[21] due to its local character. In contrast, for the composites with 70 and 80 wt % PEO, where excess PEO exists outside the galleries, both the α- and β-processes are observed almost identical to those of pure PEO. This α-process is due to the segmental motion of the amorphous regions of the PEO chains that reside outside the galleries and crystallize similarly to bulk PEO. The α'-process, with dynamics intermediate between the α- and β-processes, is observed in these systems as well, with Arrhenius dependence and a dielectric strength that is an increasing function of the clay content, i.e., of the ratio of confined to unconfined chains. The process is due to PEO confined within the galleries. The activation energies of the α'-process vary from 28 $\pm$ 3 kJ/mol for the 80 wt % to 17 $\pm$ 2 kJ/mol for the 70 wt %, 13 $\pm$ 3 kJ/mol for the 50 wt %, and 12 $\pm$ 2 kJ/mol for the 30 wt % in PEO.

The main finding on the effect of confinement on polymer mobility is the appearance of a dielectric process, intermediate between the α- and β-processes, which exhibits Arrhenius temperature dependence. For low PEO content, the PEO chains are intercalated within the galleries and the single α'-process reflects the accelerated segmental dynamics. For high PEO content (above 50 wt %), a fraction of the PEO chains are intercalated with the remaining chains residing outside the galleries and being able to crystallize. The coexisting α- and α'-processes originate from the unconfined and confined amorphous PEO segments, respectively (PEO segments lying in the vicinity of the outer clay surface may also contribute to the α'-process[22,23]).

In addition to the polymer mobility, the effect of confinement on the ionic mobility is investigated. It is well-known that the negatively charged silicate sheets contain charge-compensating

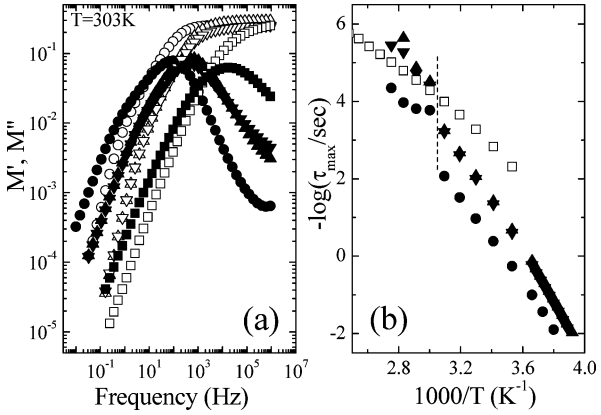

Figure 4. (a) Real (○, △, ▽, □) and imaginary (●, ▲, ▼, ■) parts of the electric modulus at 303 K for pure PEO (○, ●) and PEO/Na^+-MMT composites with 95 wt % (△, ▲), 80 wt % (▽, ▼), and 50 wt % (□, ■) weight fraction of PEO. (b) Temperature dependence of the ionic relaxation times of the samples in (a) with the vertical line denoting the T_m of bulk PEO.

mobile cations (Na^+) within the galleries. Figure 4a shows the real and imaginary parts of the electric modulus for bulk PEO and for three PEO/Na^+MMT nanocomposites. The characteristic relaxation times of the conductivity relaxation, obtained from the maximum of M'' and shown in Figure 4b, display the common VFT dependence and a characteristic speed-up at the bulk melting temperature, T_m, for all samples with excess PEO outside the galleries; no jump is observed for the 50 wt % composite where the PEO does not crystallize. When compared under isothermal conditions, the presence of Na^+MMT clay promotes ion transport both below and above the bulk T_m, and the higher the percentage of confined PEO, the faster is the ion mobility. This should be related to the noncrystalline structure of the confined PEO.[24] It is noted that computer simulations of PEO/Li^+MMT intercalates[19] showed that the ion hopping through the local energy minima of the MMT surface is assisted by the faster PEO segmental motion, thus enhancing ionic mobility.

The effect of confinement will, in general, depend on the way monomers pack near a "wall" and on the strength of the monomer−wall interactions. Simulations show[25] that chains adopt a preferentially parallel configuration near a wall with oscillations in the monomer density profile, which lead to enhanced monomeric mobilities extending over distances, which increase with supercooling in excess of the chain dimensions. Under severe confinement this "interphase" may extend over the whole film, thus leading to faster relaxation. Alternatively, the argument of a characteristic length scale ξ of cooperatively rearranging regions has been invoked in studies of low-molecular-weight glass-formers and polymers. Within this argument one may think that at very high temperatures ξ is smaller than the interlayer spacing d; thus, no difference can be expected between bulk and confined PEO. As temperature decreases, the bulk dynamics deviate from the Arrhenius dependence at the onset of cooperativity and ξ increases unhindered. Thus, the bulk dynamics can be increasingly retarded compared to that within the galleries, where d places a limit on ξ. This qualitative argument is supported by quantitative comparisons of the data for the confined PMPS[15] with the primitive relaxation time of Ngai's coupling model.[26]

The Arrhenius dependence of the α'-process in PEO/Na^+-MMT should be contrasted with the VFT one of the fast process in confined PMPS.[15] This may reflect that bulk PEO is less fragile than PMPS with a steepness index m (= d[log$\tau(T_g)$]/

$d(T_g/T)$ at $\tau(T = T_g) \cong 1$ s) of 22 compared to 73 for PMPS. Second, it may be due to the different intermolecular cooperativities of PEO and PMPS: PEO, with the small monomeric volume and flexible backbone, is expected to be predominantly intramolecularly cooperative[27] whereas PMPS, bearing a bulky side chain, more intermolecularly cooperative.[28] Thus, $\xi_{PEO} < \xi_{PMPS}$, giving rise to the observed Arrhenius dependence.

In conclusion, it is shown that the main effect of the confinement of PEO within the silicate layers is to significantly enhance the segmental mobility expressed via the α'-process with an Arrhenius temperature dependence and a single activation energy. Moreover, increased ionic mobility compared to that of bulk PEO was observed. The results are discussed on the basis of current views on local dynamics in confinement within both the cooperativity arguments and the layering ideas.

Acknowledgment. This work was partially supported by the Greek General Secretariat of Research and Technology (PENED Programme) and by the Greek Ministry of Education (Pythagoras and Applied Molecular Spectroscopy postgraduate program).

References and Notes

(1) Forrest, J. E.; Jones, R. A. L. In *Polymer Surfaces, Interfaces and Thin Films*; Karim, A., Kumar, S., Eds.; World Scientific: Singapore, 2000. Forrest, J. A.; Dalnoki-Veress, K. *Adv. Colloid Interface Sci.* **2001**, *94*, 167.

(2) Special Issue on "Properties of thin polymer films". Reiter, G., Forrest, J. A., Eds. [*Eur. Phys. J. E* **2002**, *8*, 101−266].

(3) Huwe, A.; Kremer, F. In *Liquid Dynamics. Experiments, Simulation and Theory*; Fourkas, J. T., Ed.; *ACS Symp. Ser.* **2002**, *820*, 268−283.

(4) Special Issue on "Dynamics in Confinement". Frick, B.; Koza, M.; Zorn, R., Eds. [*Eur. Phys. J. E* **2003**, *12*, 5−194].

(5) Alcoutlabi, M.; McKenna, G. B. *J. Phys.: Condens. Matter* **2005**, *17*, R461. Roth, C. B.; Dutcher, J. R. *J. Electroanal. Chem.* **2005**, *584*, 13.

(6) Sharp, J. S.; Forrest, J. A. *Phys. Rev. Lett.* **2003**, *91*, 235701.

(7) Ellison, C. J.; Torkelson, J. M. *Nat. Mater.* **2003**, *2*, 695.

(8) Sakaki, T.; Shimizu, A.; Mourey, T. H.; Thurau, C. T.; Ediger, M. D. *J. Chem. Phys.* **2003**, *119*, 8730.

(9) Ash, B. J.; Siegel, R. W.; Schadler, L. S. *J. Polym. Sci., Part B: Polym. Phys.* **2004**, *42*, 4371.

(10) Bansal, A.; Yang, H.; Li, C.; Cho, K.; Benicewicz, B. C.; Kumar, S. K.; Schadler, L. S. *Nat. Mater.* **2005**, *4*, 693.

(11) Giannelis, E. P. *Adv. Mater.* **1996**, *8*, 29. Krishnamoorti, R. K.; Vaia, R. A.; Giannelis, E. P. *Chem. Mater.* **1996**, *8*, 1728.

(12) Giannelis, E. P.; Krishnamoorti, R. K.; Manias, E. *Adv. Polym. Sci.* **1999**, *138*, 107.

(13) Wong, S.; Vaia, R. A.; Giannelis, E. P.; Zax, D. B. *Solid State Ionics* **1996**, *86*, 547.

(14) Vaia, R.; Sauer, B. B.; Tse, O. K.; Giannelis, E. P. *J. Polym. Sci., Part B: Polym. Phys.* **1997**, *35*, 59.

(15) Anastasiadis, S. H.; Karatasos, K.; Vlachos, G.; Manias, E.; Giannelis, E. P. *Phys. Rev. Lett.* **2000**, *84*, 915.

(16) Zax, D. B.; Yang, D.-K.; Santos, R. A.; Hegemann, H.; Giannelis, E. P.; Manias, E. *J. Chem. Phys.* **2000**, *112*, 2945. Manias, E.; Giannelis, E. P.; Zax, D. B.; Anastasiadis, S. H. *Polym. Mater. Sci. Eng.* **2000**, *82*, 259.

(17) Frick, B.; et al. *J. Non-Cryst. Solids* **2005**, *351*, 2657.

(18) Vaia, R. A.; Vasudevan, S.; Krawiec, W.; Scanlon, L. G.; Giannelis, E. P. *Adv. Mater.* **1995**, *7*, 154.

(19) Hackett, E.; Manias, E.; Giannelis, E. P. *Chem. Mater.* **2000**, *12*, 2161. Kuppa, V.; Manias, E. *Chem. Mater.* **2002**, *14*, 2171.

(20) The relaxation times obtained from the electric modulus (τ_{M^*}) and those from the complex permittivity (τ_{ϵ^*}) may differ as $\tau_{M^*}/\tau_{\epsilon^*} \sim \epsilon_\infty/\epsilon_0$ (ϵ_0 and ϵ_∞ are the values of ϵ at low and high frequencies).

(21) The apparently altered dynamics of the β-process for the 50 wt % nanocomposite at high frequencies is due to traces of water. This finding is supported by extensive studies of nanocomposites in the presence of traces of water (not shown herein). This relaxes with a rate comparable to the high-temperature PEO/Na^+MMT β-process and causes the peculiar $\tau(T)$ dependence at higher temperatures.

(22) A similar process with fast dynamics was observed in semicrystalline bulk PEO and was attributed to the motion of PEO segments confined in the transition region between PEO lamellae and interlamellar amorphous regions [Jin, X.; Zhang, S.; Runt, J. *Polymer* **2002**, *43*, 6247]. Moreover, PVME segments constrained by the matrix of frozen majority PS chains in polystyrene/poly(vinyl methyl ether), PS/PVME, blends appear to move with a similar process exhibiting Arrhenius dependence [Lorthioir, C.; Alegría, A.; Colmenero, J. *Phys. Rev. E* **2003**, *68*, 031805]. This may also be related to the dynamics of the so-called "rigid amorphous fraction" studied by Wunderlich [Wunderlich, B.; Androsch, R. *Polymer* **2005**, *46*, 12556. Pyla, M.; Nowak-Pyda, E.; Heeg, J.; Huth, H.; Minakov, A. A.; Di Lorenzo, M. L.; Schick, C.; Wunderlich, B. *J. Polym. Sci., Part B: Polym. Phys.* **2006**, *44*, 1364].

(23) In certain cases, new processes related to modifications of the normal mode (chain relaxation) upon confinement have been observed for polyisoprene (type A) chains [Petychakis, L.; Floudas, G.; Fleischer, G. *Europhys. Lett.* **1997**, *40*, 685. Serghei, A.; Kremer, F. *Phys. Rev. Lett.* **2003**, *91*, 165702. Mijović, J.; Lee, H.; Kenny, J.; Mays, J. *Macromolecules* **2006**, *39*, 2172]. Finally, an extra process was obtained in thin films attributed to the segmental motion in a liquidlike surface layer [Fukao, K.; Miyamoto, Y. *Phys. Rev. E* **2000**, *61*, 1743].

(24) Croce, F.; Appetecchi, G. B.; Persi, L.; Scrosati, B. *Nature (London)* **1998**, *394*, 456.

(25) Mischer, C.; Baschnagel, J.; Binder, K. *Adv. Colloid Interface Sci.* **2001**, *94*, 197. Baschnagel, J.; Varnik, F. *J. Phys.: Condens. Matter* **2005**, *17*, R851.

(26) Ngai, K. L. *Philos. Mag. B* **2002**, *82*, 291.

(27) Floudas, G.; Mpoukouvalas, K.; Papadopoulos, P. *J. Chem. Phys.* **2006**, *124*, 074905.

(28) Roland, C. M.; Hensel-Bielowka, S.; Paluch, M.; Casalini, R. *Rep. Prog. Phys.* **2005**, *68*, 1405. Ngai, K. L.; Roland, C. M. *Macromolecules* **1993**, *26*, 6824.

MA0608368